Supplement of Atmos. Chem. Phys., 19, 5021–5032, 2019
https://doi.org/10.5194/acp-19-5021-2019-supplement

Atmospheric Chemistry and Physics
Open Access
EGU

Supplement of

Aqueous reactions of organic triplet excited states with atmospheric alkenes

Richie Kaur et al.

Correspondence to: Cort Anastasio (canastasio@ucdavis.edu)

Table S1. Reference probes and triplicate measurements of rate constants for alkenes in a solution at pH 5.5. Errors (in parentheses) for each replicate measurement represent ± 1 standard error, determined by propagating errors in the slope of the relative rate plot and in the reference compound rate constant. Errors on the average values represent ± 1 σ determined from the average of the replicate values.

#	Alkene Name (ALK)	Abbreviation	Reference Probe	$k_{ALK+3BP*}$ (10^8 M^{-1} s^{-1})			
				Replicate 1	Replicate 2	Replicate 3	Average (SD)
1	5-Hexen-1-ol	5HxO	3MBO	3.1 (0.4)	1.9 (0.3)	2.2 (0.3)	2.4 (0.6)
2	Allyl alcohol	AlO	BDO	2.8 (0.3)	2.5 (0.2)	2.8 (0.3)	2.7 (0.2)
3	3-Hexene-1,6-diol	HDO	3MBO	2.5 (0.4)	3.7 (0.5)	3.2 (0.4)	3.1 (0.7)
4	2,3-Butadien-1-ol	BDO	3MBO	3.3 (0.5)	3.8 (0.5)	3.6 (0.5)	3.6 (0.3)
5	3-Buten-1-ol	3B1O	cHxO	4.2 (0.4)	3.2 (0.3)	3.6 (0.4)	3.7 (0.5)
6	1-Penten-3-ol	PE3O	3B2O	3.9 (1.1)	4.2 (1.2)	4.7 (1.3)	4.3 (0.4)
7	3-Buten-2-ol	3B2O	cHxO	5.7 (0.5)	5.6 (0.5)	3.3 (0.5)	4.9 (1.3)
8	2-Buten-1-ol	2B1O	4M3PO	5.6 (0.2)	4.1 (0.3)	5.9 (0.5)	5.2 (1.0)
9	5-Hexenyl acetate	5HxAc	3MBO	4.7 (0.7)	5.0 (0.7)	7.9 (1.1)	5.9 (1.8)
10	trans-3-hexen-1-ol	tHxO	3MBO	13 (2)	14 (2)	14 (2)	14 (1)
11	1-Chloro-3-methyl-2-butene	CMB	BDO [a]	17 (1)	-	-	17 (1)[b]
12	3-Methyl-2-buten-1-ol	3MBO	cHxO	21 (2)	20 (2)	16 (1)	19 (3)
13	2-Methyl-2-penten-1-ol	2M2PO	3MBO	29 (4)	28 (4)	28 (4)	28 (1)
14	4-Methyl-3-penten-1-ol	4M3PO	3MBO	42 (6)	39 (5)	40 (5)	40 (2)
15	cis-3-hexen-1-ol	cHxO	PhOH	62 (11) [c]	70 (13)	59 (11)	64 (6)
16	cis-3-hexenyl acetate	cHxAc	cHxO	66 (7)	71 (6)	59 (5)	65 (6)
17	Methyl jasmonate	MeJA	cHxO	80 (7)	69 (6)	75 (7)	75 (5)

[a] Measurement of the rate constant for CMB was done in a solution containing a minimal amount of acetonitrile to dissolve the compound.

[b] Error represents ± 1 SE, based on the SE of the relative rate slope and reference rate constant $k_{BDO+3BP*}$ given in the table.

[c] Phenol (PhOH) was used as the reference probe using the reference rate constant of 3.9 (± 0.7) × 10^9 M^{-1} s^{-1}, measured in this study, using 2,4,6,-trimethylphenol (TMP) as a reference compound ($k_{TMP+3BP*}$ = 5.1 (± 0.9) × 10^9 M^{-1} s^{-1}; Canonica et al. (2000)).

Table S2. Highest- and singly-occupied molecular orbitals (HOMOs, SOMOs) of representative alkenes showing removing of an electron from the π system.[†]

ALK Abbreviation (#)	HOMO	SOMO	HOMO+1 (eV)	SOMO+1 (eV)
HDO (3)	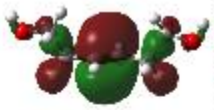		 0.39	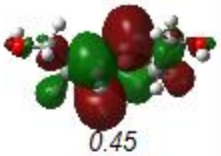 0.45
BDO (4)			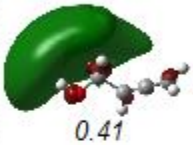 0.41	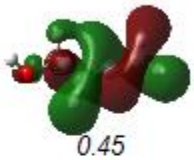 0.45
PE3O (6)		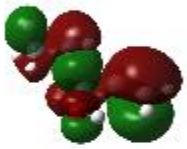	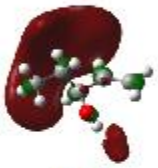 0.41	 0.49
3B2O (7)	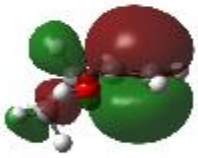		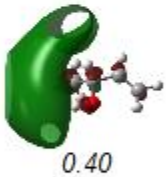 0.40	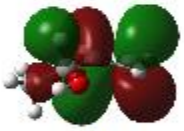 0.49
3MBO (12)	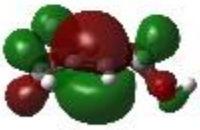		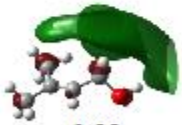 0.38	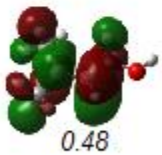 0.48
cHxO (15)	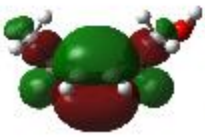		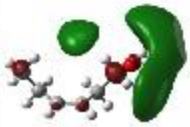 0.39	 0.46

[†] HOMOs and SOMOs were computed from single point calculations at MP2/CBSB3 (Frisch et al., 2016). HOMO+1 and SOMO+1values in eV are shown relative to HOMO and SOMO, respectively.

Table S3. HOMOs and SOMOs of alkenes showing removing of an electron from the oxygen.[†]

ALK Abbreviation (#)	HOMO	SOMO	HOMO+*1* *(eV)*	SOMO+*1* *(eV)*
3B1O (5)	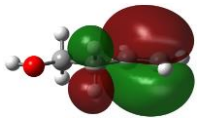	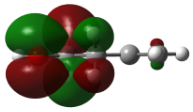	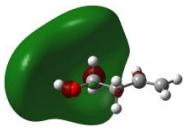 *0.40*	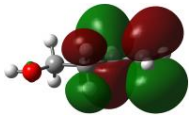 *0.45*
HxAc (16)	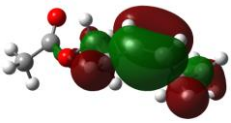	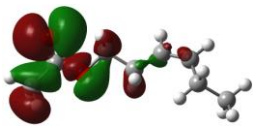	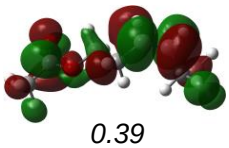 *0.39*	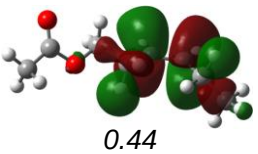 *0.44*
MeJA (17)	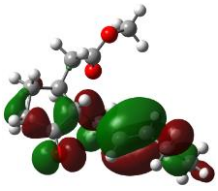	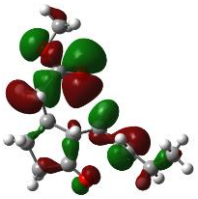	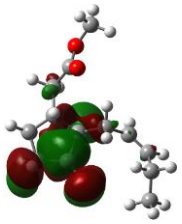 *0.37*	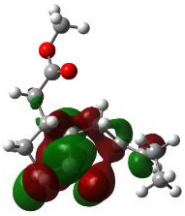 *0.19*

[†]HOMOs and SOMOs were computed from single point calculations at MP2/CBSB3 (B3LYP/CBSB7 was used for ALKs **16** and **17**). HOMO+1 and SOMO+1 values in eV are shown relative to HOMO and SOMO, respectively.

Table S4. Oxidation potentials (in units of V) of various isomers of isoprene- and limonene-derived OVOCs, calculated using the CBS-QB3 compound method. The lowest energy isomer for each OVOC is highlighted using a blue box. Compounds not shown here (18, 20 and 22) have no relevant isomers.

δ4 ISOPOOH (19)	δISONO2 (21)	LMNALD (23)	2,5OH-LMNALD (24)		4,7OH-LMNALD (25)
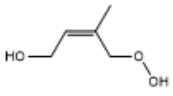 2.25	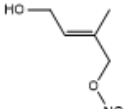 2.40	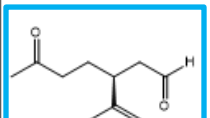 2.22	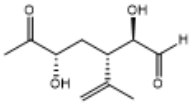 2.06	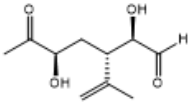 2.24	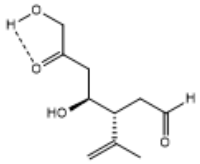 2.17
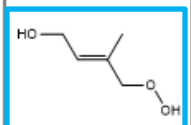 2.28	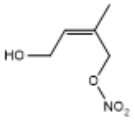 2.45	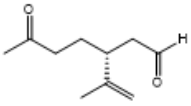 2.28	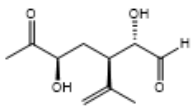 2.12	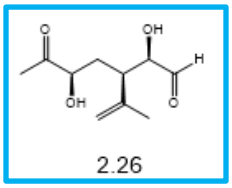 2.26	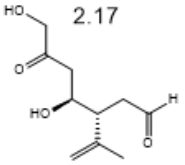 2.17
			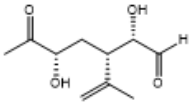 2.23	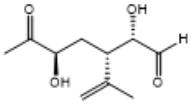 2.39	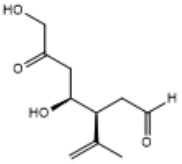 2.21
			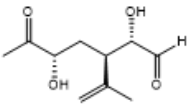 2.24	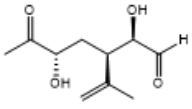 2.39	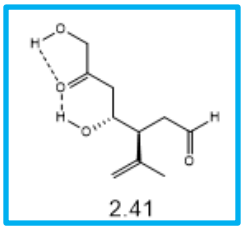 2.41
					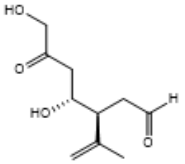 2.48

Table S5. Measured or estimated rate constants for reactions of OVOCs with oxidants, photolysis, and hydrolysis.

OVOC		Gas-phase rate constants (cm^3 mlc^{-1} s^{-1})					
#	Name	$k_{OVOC+OH}$	Reference	$k_{OVOC+O3}$	Reference	$j_{Photolysis}$ (s^{-1})	Reference
18	β4-ISOPOOH	1.2E-10	St. Clair et al. (2015)	1.3E-17	Khamaganov and Hites (2001)		
19	δ4-ISOPOOH	1.2E-10	St. Clair et al. (2015)	1.3E-17	Khamaganov and Hites (2001)		
20	β-ISONO2	5.4E-11	Lee et al. (2014)	5.0E-19	Lee et al. (2014)		
21	δ-ISONO2	1.1E-10	Lee et al. (2014)	2.8E-17	Lee et al. (2014)		
22	HPALD2	5.1E-11	Wolfe et al. (2012)	1.2E-18	Wolfe et al. (2012)	6.3E-05	Wolfe et al. (2012)
23	LMNALD	1.6E-10	Gill and Hites (2002)	2.1E-16	Khamaganov and Hites (2001)		
24	2,5OH-LMNALD	1.6E-10	Gill and Hites (2002)	2.1E-16	Khamaganov and Hites (2001)		
25	4,7OH-LMNALD	1.6E-10	Gill and Hites (2002)	2.1E-16	Khamaganov and Hites (2001)		
26	HPALD1	5.1E-11	Wolfe et al. (2012)	1.2E-18	Wolfe et al. (2012)	6.3E-05	Wolfe et al. (2012)
OVOC		Aqueous-phase rate constants (L mol^{-1} s^{-1})					
#	Name	$k_{OVOC+OH}$	Reference	$k_{OVOC+O3}$	Reference	$k'_{Hydrolysis}$ (s^{-1})	Reference
18	β4-ISOPOOH	2.5E+09	Rivera-Rios et al. (2018)	4.7E+04	Schöne and Herrmann (2014) [a]		
19	δ4-ISOPOOH	2.5E+09	Rivera-Rios et al. (2018)	4.7E+04	Schöne and Herrmann (2014) [a]		
20	β-ISONO2	5.0E+09	Herrmann et al. (2015) [b]	4.7E+04	Schöne and Herrmann (2014) [a]	1.6E-05	Jacobs et al. (2014)
21	δ-ISONO2	5.0E+09	Herrmann et al. (2015) [b]	4.7E+04	Schöne and Herrmann (2014) [a]	6.8E-03	Jacobs et al. (2014)
22	HPALD2	9.0E+09	Schöne et al. (2014) [c]	2.3E+04	Schöne and Herrmann (2014) [c]		
23	LMNALD	1.0E+10	Witkowski et al. (2018) [d]	4.0E+04	Witkowski et al. (2018) [d]		
24	2,5OH-LMNALD	1.0E+10	Witkowski et al. (2018) [d]	4.0E+04	Witkowski et al. (2018) [d]		
25	4,7OH-LMNALD	1.0E+10	Witkowski et al. (2018) [d]	4.0E+04	Witkowski et al. (2018) [d]		
26	HPALD1	9.0E+09	Schöne et al. (2014) [c]	2.3E+04	Schöne and Herrmann (2014) [c]		

[a] Average of rate constants for methacrolein and methyl vinyl ketone used as a proxy.
[b] Estimate based on the rate constants for similar unsaturated compounds with •OH in the indicated reference.
[c] Rate constant for methacrolein used as a proxy.
[d] Rate constants for neutral dicarbonyl derivatives of limonic and limononic acids, used a proxies.

Table S6. Loss rate constants for OVOCs due to different pathways.

#	OVOC Name	K_H [a] ($M\ atm^{-1}$)	χ_{aq} [b]	Pseudo-first-order rate constant for loss due to oxidants in the gas-phase (s^{-1})			Pseudo-first-order rate constant for loss due to oxidants in the aqueous-phase (s^{-1})				
				$k'_{OH,g}$ [c]	$k'_{O3,g}$ [d]	j_{hv} [e]	$k'_{OH,aq}$ [f]	$k'_{O3,aq}$ [g]	$k'_{3BP*,aq}$ [h] (High Triplet Reactivity)	$k'_{3C*,aq}$ [i] (Typical Triplet Reactivity)	k'_{Hyd} [j]
18	β4-ISOPOOH	1.5E+06	0.97	1.2E-04	9.6E-06		5.0E-06	1.6E-05	4.0E-06	1.4E-07	
19	δ4-ISOPOOH	1.2E+06	0.97	1.2E-04	9.6E-06		5.0E-06	1.6E-05	6.8E-05	2.4E-06	
20	β-ISONO2	5.1E+04	0.55	5.4E-05	3.7E-07		1.0E-05	1.6E-05	2.1E-05	7.3E-07	1.6E-05
21	δ-ISONO2	4.3E+04	0.51	1.1E-04	2.1E-05		1.0E-05	1.6E-05	4.6E-05	1.6E-06	6.8E-03
22	HPALD2	1.2E+05	0.75	5.1E-05	8.9E-07	6.3E-05	1.8E-05	7.6E-06	2.0E-05	7.0E-07	
23	LMNALD	4.5E+03	0.10	1.6E-04	1.6E-04		2.0E-05	1.3E-05	8.3E-05	2.9E-06	
24	2,5OH-LMNALD	8.0E+05	0.95	1.6E-04	1.6E-04		2.0E-05	1.3E-05	7.3E-05	2.6E-06	
25	4,7OH-LMNALD	8.0E+05	0.95	1.6E-04	1.6E-04		2.0E-05	1.3E-05	4.4E-05	1.6E-06	
26	HPALD1	1.2E+05	0.75	5.1E-05	8.9E-07	6.3E-05	1.8E-05	7.6E-06	- [k]	- [k]	

[a] Henry's law constants calculated using EPISuite version 4.1 (US EPA. Estimation Programs Interface Suite™ for Microsoft® Windows v 4.1, 2016).

[b] Fraction of OVOC in the aqueous phase, calculated as $\chi_{aq} = 1/(1+1/(K_H \times L \times R \times T))$, where K_H is the Henry's law constant of the OVOC, L is the assumed liquid water content (1×10^{-6} L-aq/L-g), R is the universal gas constant (0.082 L atm K^{-1} mol^{-1}), and T = 298 K.

[c,d,f,g,h,i] Pseudo-first-order rate constant for loss of OVOC due to oxidation by the given oxidant in the gas or aqueous phase, calculated by multiplying the bimolecular reaction rate constant (Table S6) with the corresponding steady-state concentration of the oxidant: [$^{\bullet}$OH(g)] = 1×10^6 molecules cm^{-3}, [O_3(g)] = 30 ppbv = 7.4×10^{11} molecules cm^{-3}, [$^{\bullet}$OH(aq)] = 2×10^{-15} M (estimate in typical fog drops, includes gas-to-aqueous partitioning, Kaur and Anastasio (2017)). [O_3(aq)] = 3.3×10^{-10} M (based on 30 ppbv O_3(g) and $K_H = 1.1 \times 10^{-2}$ M atm^{-1}; Seinfeld and Pandis (2012), and [^{3}C*(aq)] = 5×10^{-14} M (average concentration measured in Davis fog, Kaur and Anastasio (2017)).

[h] Pseudo-first-order rate constant for loss of OVOC due to oxidation by highly reactive triplets such as ^{3}BP*. This was calculated using the predicted second-order rate constants $k_{OVOC+3BP*}$ (Table 1, main text) and [^{3}C*(aq)] given in the footnote above.

[i] Pseudo-first-order rate constant for loss of OVOC due to oxidation by triplets of typical reactivity as measured in fog and particles in Davis, CA (Kaur and Anastasio, 2017; Kaur and Anastasio, 2018). To estimate these rate constants we multiplied the predicted second-order rate constants with ^{3}BP* ($k_{OVOC+3BP*}$) by a factor of 0.04, which is the ratio of the average of the rate constants of reaction of MeJA with ^{3}3MAP* and ^{3}DMB* (2.7×10^8 M^{-1} s^{-1}, Table S8) divided by the rate constant for MeJA with ^{3}BP* (7.5×10^9 M^{-1} s^{-1}, Tables S1 and S8).

[e, j] First-order rate constants for gas-phase photolysis and aqueous hydrolysis of the OVOC, respectively (also given in Table S5).

[k] The value of $k_{ALK+3BP*}$ for HPALD1 could not be determined due to challenges with calculating its oxidation potential. Because the CB3-QB3 method scales at N^7 (where N is the number of atoms), the larger compound required more computational power than available.

Table S7. OVOC lifetimes and fractions lost due to various pathways.

High Triplet Reactivity Scenario		Total		Fraction of OVOC lost due to each pathway [c]						
#	OVOC Name	k'_{OVOC} [a] (s^{-1})	τ [b] (h)	$^{\bullet}OH(g)$	$O_3(g)$	hν(g)	$^{\bullet}OH(aq)$	$O_3(aq)$	$^3BP^*(aq)$	Hyd(aq)
18	β4-ISOPOOH	2.7E-05	10	13%	1.0%	0%	18%	54%	14%	0%
19	δ4-ISOPOOH	9.0E-05	3.1	3.9%	0.32%	0%	5.4%	17%	74%	0%
20	β-ISONO2	5.9E-05	4.7	41%	0.28%	0%	9.4%	15%	19%	15%
21	δ-ISONO2	3.6E-03	0.078	1.5%	0.29%	0%	0.14%	0.22%	0.66%	97%
22	HPALD2	6.3E-05	4.4	20%	0.35%	25%	21%	9.1%	24%	0%
23	LMNALD	3.0E-04	0.93	49%	47%	0%	0.67%	0.44%	2.8%	0%
24	2,5OH-LMNALD	1.2E-04	2.4	6.9%	6.7%	0%	16%	11%	59%	0%
25	4,7OH-LMNALD	8.9E-05	3.1	9.0%	8.8%	0%	21%	14%	47%	0%
26	HPALD1	4.8E-05	5.8	27%	0.46%	33%	28%	12%	- [d]	0%
Typical Triplet Reactivity Scenario		Total		Fraction of OVOC lost due to each pathway [c]						
#	OVOC Name	k'_{OVOC} (s^{-1})	τ (h)	$^{\bullet}OH(g)$	$O_3(g)$	hν(g)	$^{\bullet}OH(aq)$	$O_3(aq)$	$^3C^*(aq)$	Hyd(aq)
18	β4-ISOPOOH	2.4E-05	12	15%	1.2%	0%	20%	63%	0.58%	0%
19	δ4-ISOPOOH	2.6E-05	11	14%	1.1%	0%	19%	58%	9.0%	0%
20	β-ISONO2	4.8E-05	5.8	51%	0.43%	0%	12%	18%	0.84%	18%
21	δ-ISONO2	3.5E-03	0.079	1.5%	0.29%	0%	0.14%	0.22%	0.02%	98%
22	HPALD2	4.8E-05	5.7	26%	0.46%	33%	28%	12%	1.1%	0%
23	LMNALD	2.9E-04	1.0	50%	49%	0%	0.69%	0.45%	0.10%	0%
24	2,5OH-LMNALD	5.0E-05	5.6	16%	16%	0%	38%	25%	4.9%	0%
25	4,7OH-LMNALD	4.9E-05	5.7	16%	16%	0%	39%	26%	3.0%	0%
26	HPALD1	4.8E-05	5.8	27%	0.46%	33%	28%	12%	- [d]	0%

[a] Total pseudo-first order rate constant for loss of OVOC, calculated as $k'_{OVOC} = \Sigma(\chi_{aq} \times k'_{Ox,aq} + (1- \chi_{aq}) \times k'_{Ox,gas})$. All pseudo-first-order rate constants ($k'_{Ox,aq}$, $k'_{Ox,gas}$, $j_{hν}$, k'_{Hyd}) are given in Table S6.

[b] Total lifetime of OVOC, calculated as $1/k'_{OVOC}$.

[c] Fraction of OVOC lost due to each pathway, calculated as $(\chi_{aq} \times k'_{Ox,aq})/k'_{OVOC}$ for aqueous pathways and $((1-\chi_{aq}) \times k'_{Ox,gas})/k'_{OVOC}$ for gas-phase processes.

[d] We were unable to compute the oxidation potential for HAPLD1 (see footnote *k* in Table S6), and thus could not estimate its rate constant with triplets.

Table S8. Second-order rate constants for reaction of some alkenes with model triplet excited states.

ALK	$k_{ALK+3C*}$ 10^8 M^{-1} s^{-1}			Average ($k_{MeJA+33MAP*}$, $k_{MeJA+3DMB*}$) / $k_{MeJA+3BP*}$ [c]
	^{3}3MAP*	^{3}DMB*	^{3}BP*	
cHxO (**15**)	1.1 (± 0.2) [a]	0.24 (± 0.10) [a]	64 (± 6) [b]	0.010
cHxAc (**16**)	7.9 (± 2.0) [a]	15 (± 4) [a]	65 (± 6) [b]	0.18
MeJA (**17**)	1.2 (± 0.3) [a]	4.1 (± 1.6) [a]	75 (± 5) [b]	0.035 [d]

[a] Rate constants from Richards-Henderson et al. (2014). Listed uncertainties are ± 1 standard errors.

[b] Rate constants measured in this work (also shown in Table S1). Listed uncertainties here are ± 1 standard deviation, n = 3.

[c] The ratio of the average bimolecular rate constants for reaction of MeJA with model triplets ^{3}3MAP* and ^{3}DMB* to the rate constant for MeJA with ^{3}BP*.

[d] This is the rate constant ratio for MeJA as well as the median value of the rate constant ratio (see footnote *a*) for the three alkenes.

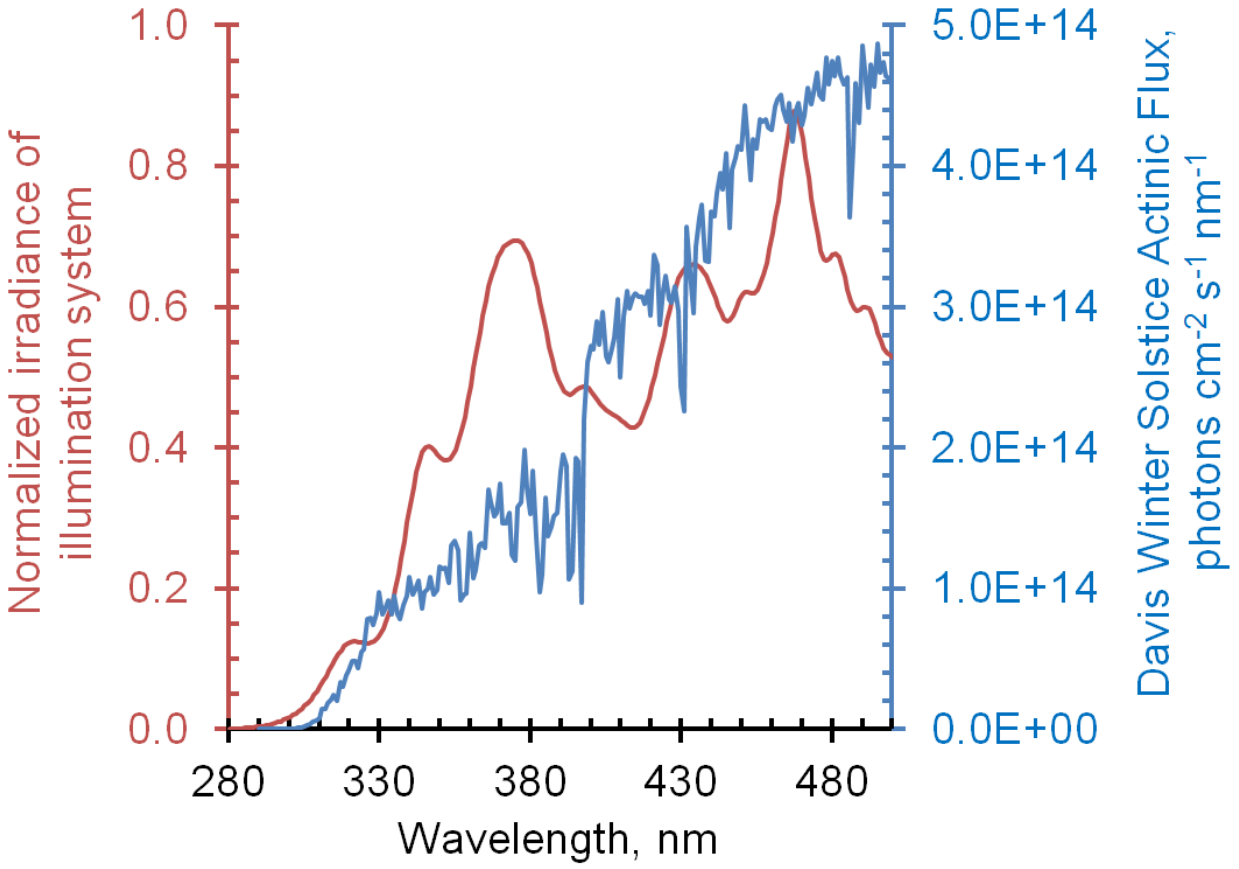

Figure S1. Comparison of the normalized irradiance from our illumination system (red line) and Davis, midday, winter solstice sunlight from the TUV model (blue line; Madronich et al. (2002)). Our illumination system irradiance was measured using a TIDAS spectrophotometer (absolute units: counts cm^{-2} nm^{-1} s^{-1}) and normalized so that the area under its curve is equal to the area under the TUV actinic flux curve. Input parameters for the TUV model were: solar zenith angle: 62°, measurement altitude: 0 km, surface albedo: 0.1, aerosol optical depth: 0.235, cloud optical depth: 0.00.

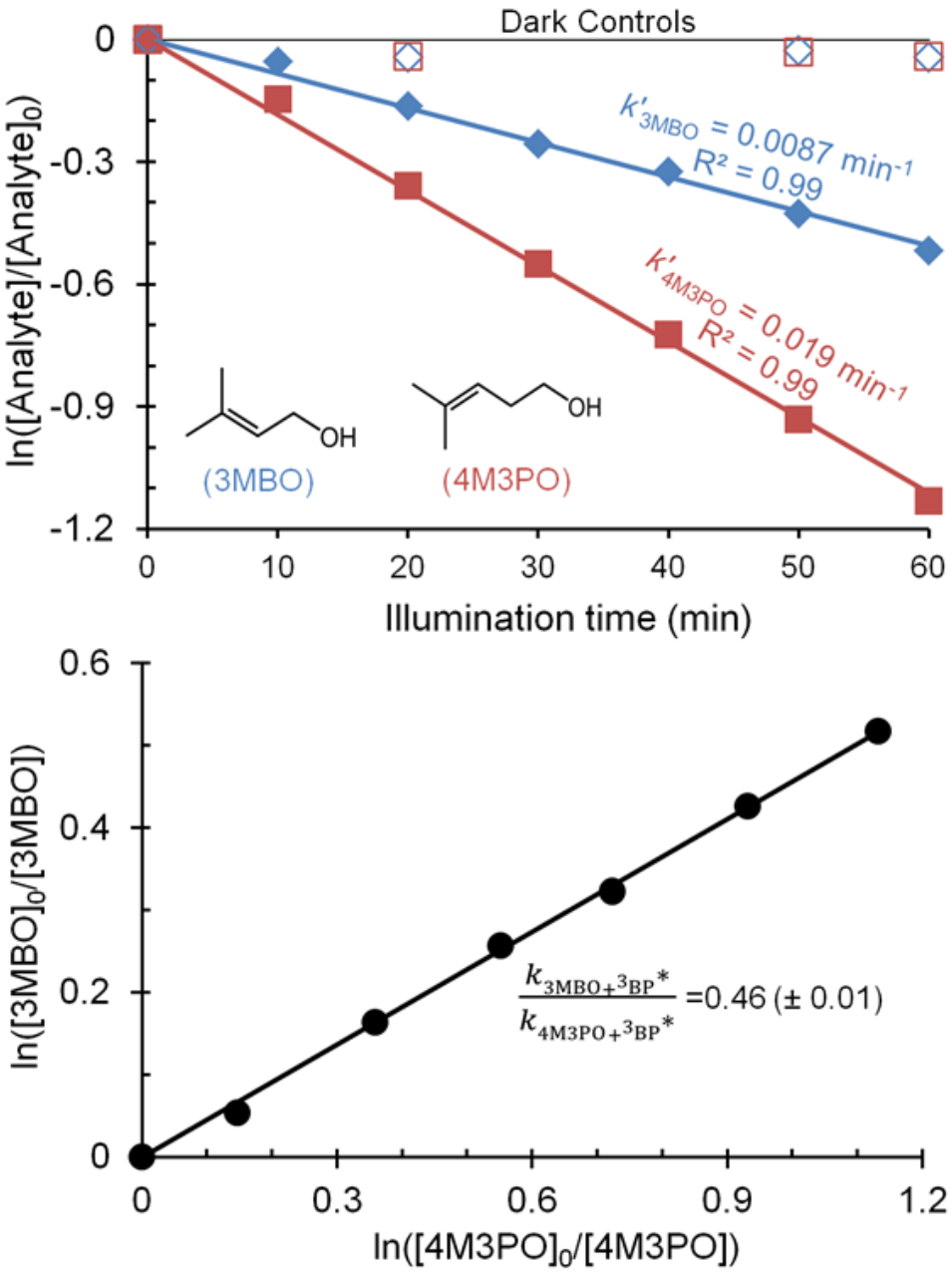

92

93 **Figure S2.** Illustration of the relative rate technique used for measuring rate constants
94 (Finlayson-Pitts and Pitts Jr, 1999; Richards-Henderson et al., 2014). Top panel: Aqueous loss of
95 the alkene (4M3PO) and reference compound (3MBO) in the presence of the BP triplet under
96 solar simulated light (298 K, pH 5.5 (± 0.2)). Bottom panel: Plot of change in concentration of
97 reference compound against alkene. The slope represents the ratio (± 1 SE) of the bimolecular
98 rate constants with the BP triplet.

99

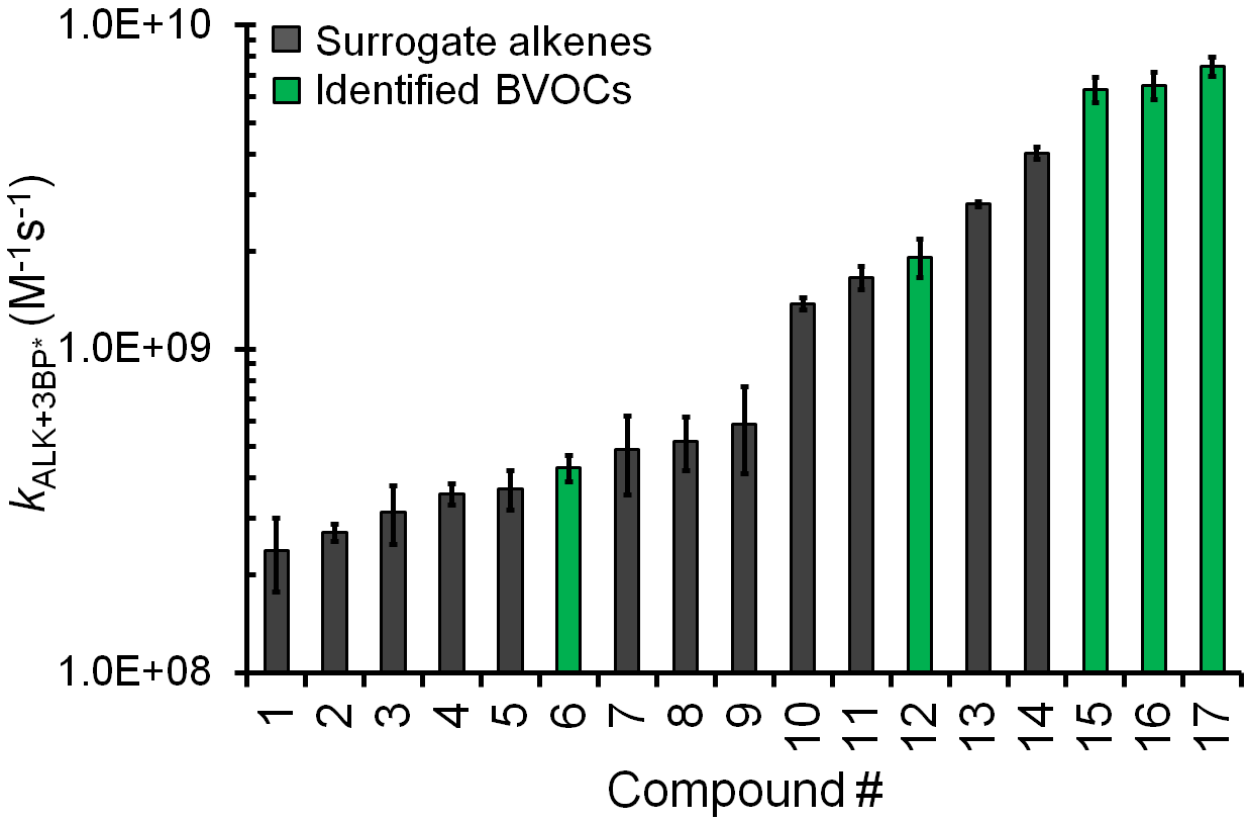

Figure S3. Measured bimolecular rate constants of 17 alkenes with triplet benzophenone. Green bars represent biogenic volatile organic compounds known to be emitted from plants; grey bars represent other C_3–C_6 alkenes. Error bars represent ±1 standard deviation (n = 3) except for compound 11, where n = 1 and the error is ± 1 SE (see Table S1 for details). Experimental conditions: 298 K, pH 5.5 ± 0.2, 1.0 mM phosphate buffer).

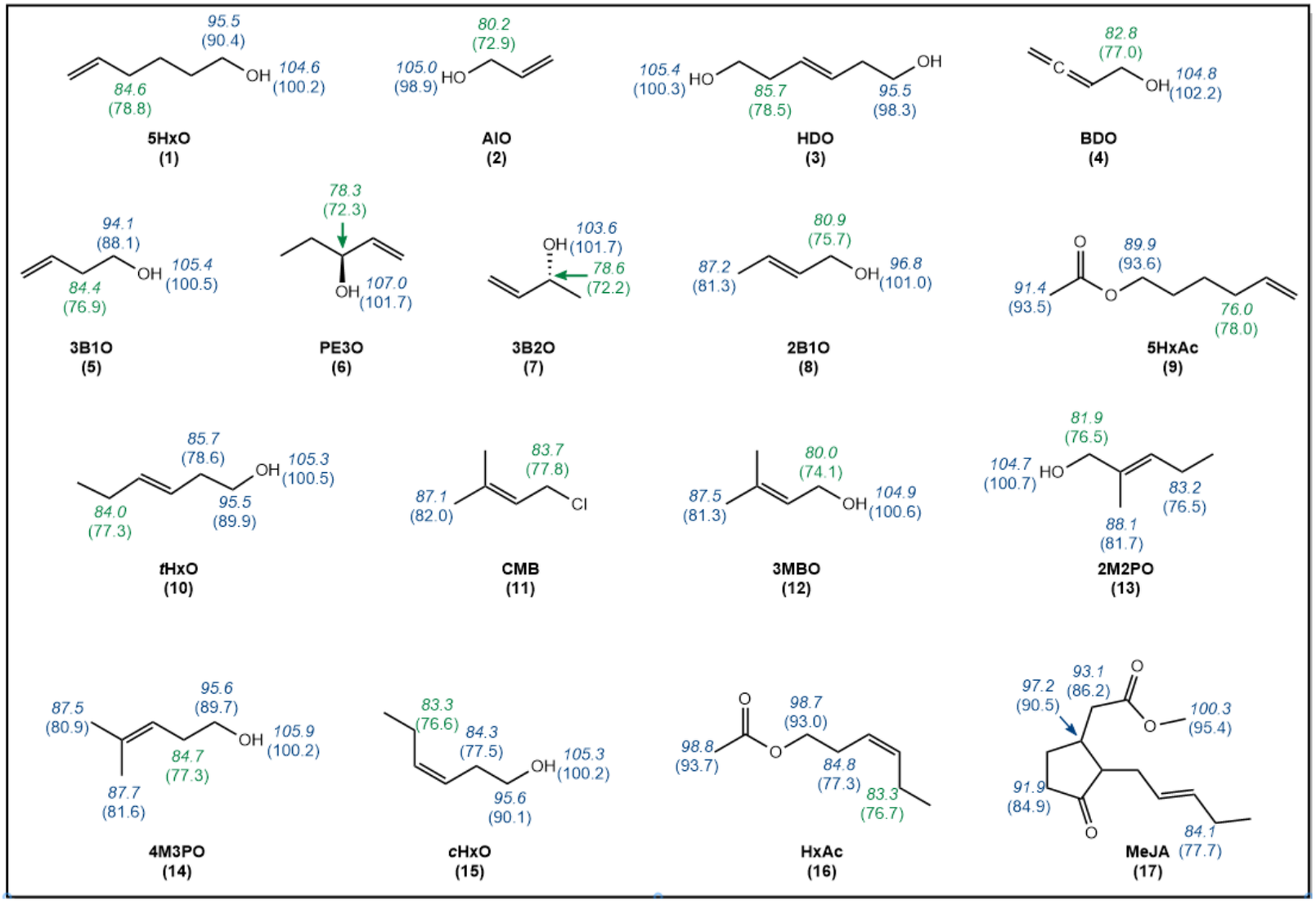

Figure S4. Bond dissociation enthalpies (in italics) and bond dissociation free energies (in parentheses) in kcal mol^{-1} for various hydrogens in each alkene. For each compound the hydrogen most likely to be abstracted, i.e., with the lowest bond dissociation energy, is shown in green.

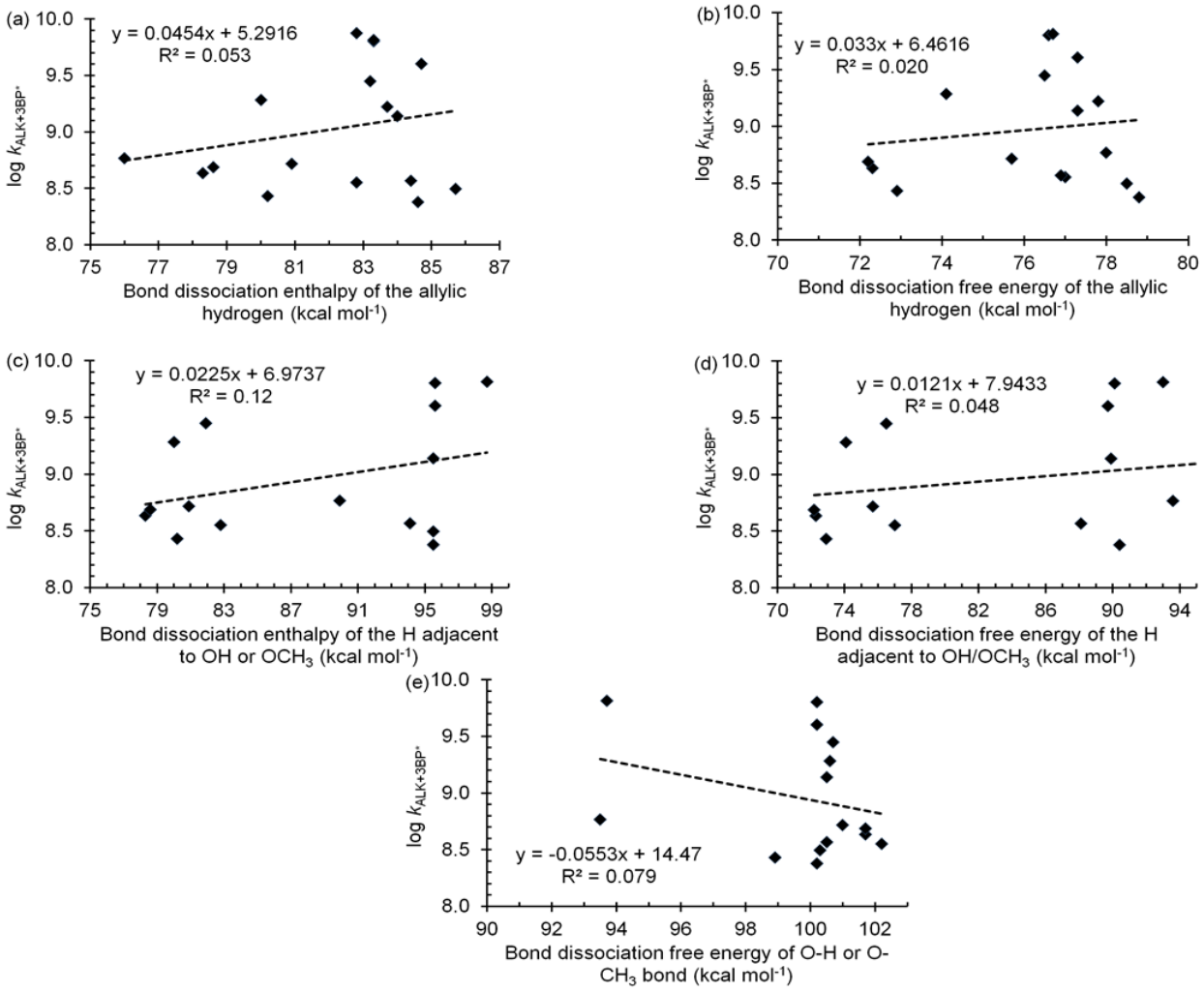

111

112 **Figure S5.** Correlation plots for measured rate constants and various computed bond dissociation
113 energies. (a) Log $k_{ALK+3BP*}$ versus the lowest bond dissociation enthalpy of the allylic hydrogen
114 in each alkene (i.e., the green values in Fig. S4). (b) Log $k_{ALK+3BP*}$ versus the lowest bond
115 dissociation free energy of the allylic hydrogen. (c) Log $k_{ALK+3BP*}$ versus the bond dissociation
116 enthalpy of the hydrogen attached to the carbon adjacent to the –OH or –OCH_3 group. (d) Log
117 $k_{ALK+3BP*}$ versus the bond dissociation free energy of the hydrogen attached to the carbon
118 adjacent to the –OH or –OCH_3 group. (e): log $k_{ALK+3BP*}$ versus bond dissociation free energy of
119 the O-H or OH_2C-H bond. Bond dissociation energies are shown in Fig. S4.

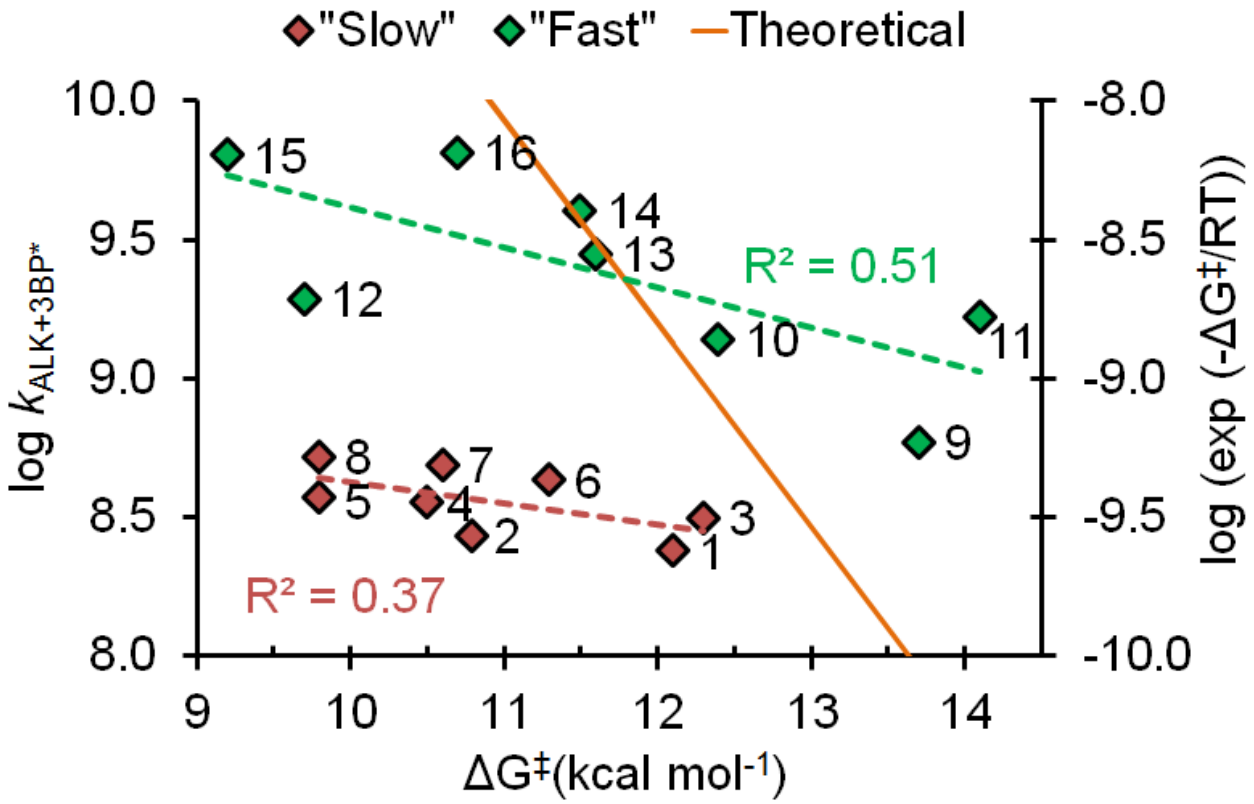

Figure S6. Log $k_{ALK+3BP*}$ versus lowest transition state free energy barrier. The alkenes are broken down into two groups: $k_{ALK+3BP*} < 5 \times 10^8$ M^{-1} s^{-1} (slow, red) and $k_{ALK+3BP*} \geq 5 \times 10^8$ M^{-1} s^{-1} (fast, green). The slopes (± 1 SE) of these lines are – 0.077 (± 0.041) and – 0.15 (± 0.06) mol $kcal^{-1}$, respectively. Transition state energy barrier values are given in Table 1 of the main text. The orange line (plotted on the secondary y-axis) shows the trend in *k* values expected from transition state theory ($k_{ALK+3BP*} = A \times \exp(-\Delta G^{\ddagger}/RT)$).

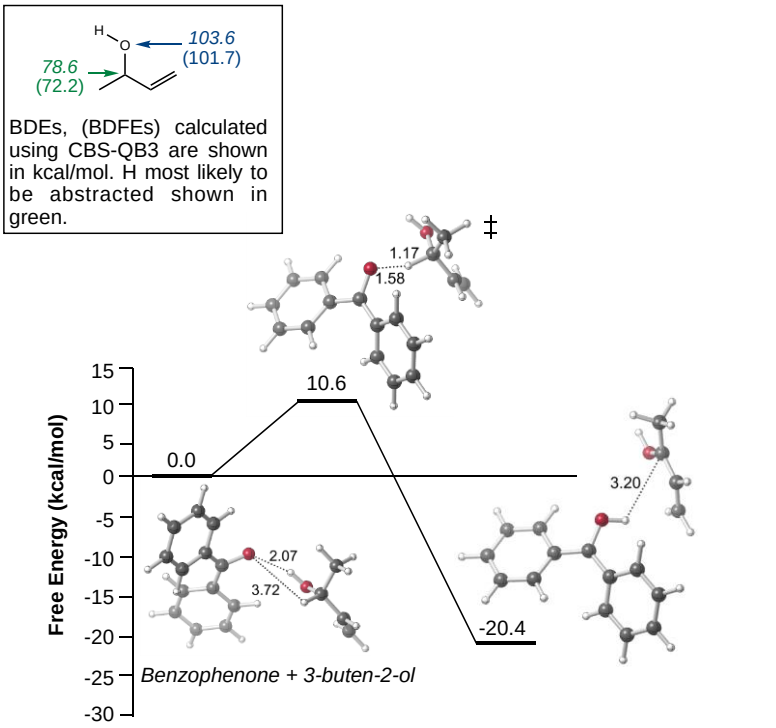

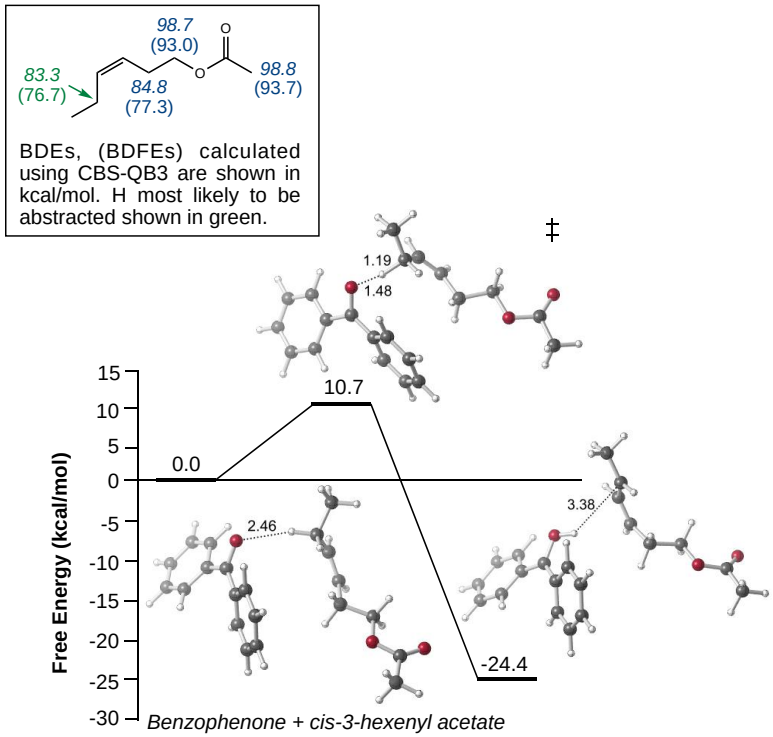

Figure S7. Lowest transition state energy barriers for two alkenes: **7**, 3B2O, in the top panel and **16**, cHxAc, in the bottom panel. Both show the hydrogen most likely to be abstracted during oxidation; in both cases this is an allylic H.

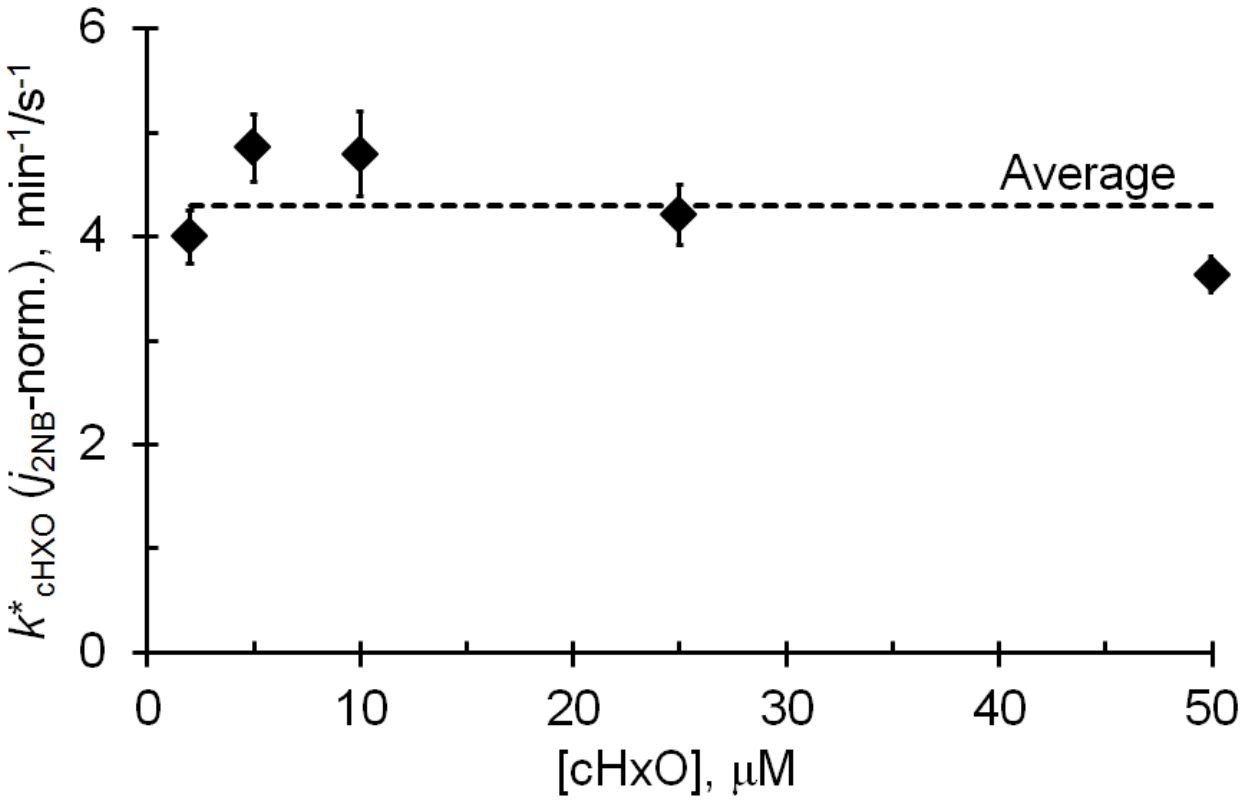

Figure S8. Pseudo-first-order loss rate constant of cHxO (k^*_{cHxO}) as a function of the concentration of cHxO. Since these experiments were performed on different days, the values are normalized to the photon flux of the illumination system on the day of the experiment by dividing by j_{2NB} (details in Kaur and Anastasio (2017))**.** The average (±1 σ) value is 4.3 ± 0.5 min^{-1}/s^{-1}, giving a relative standard deviation of 12 %.

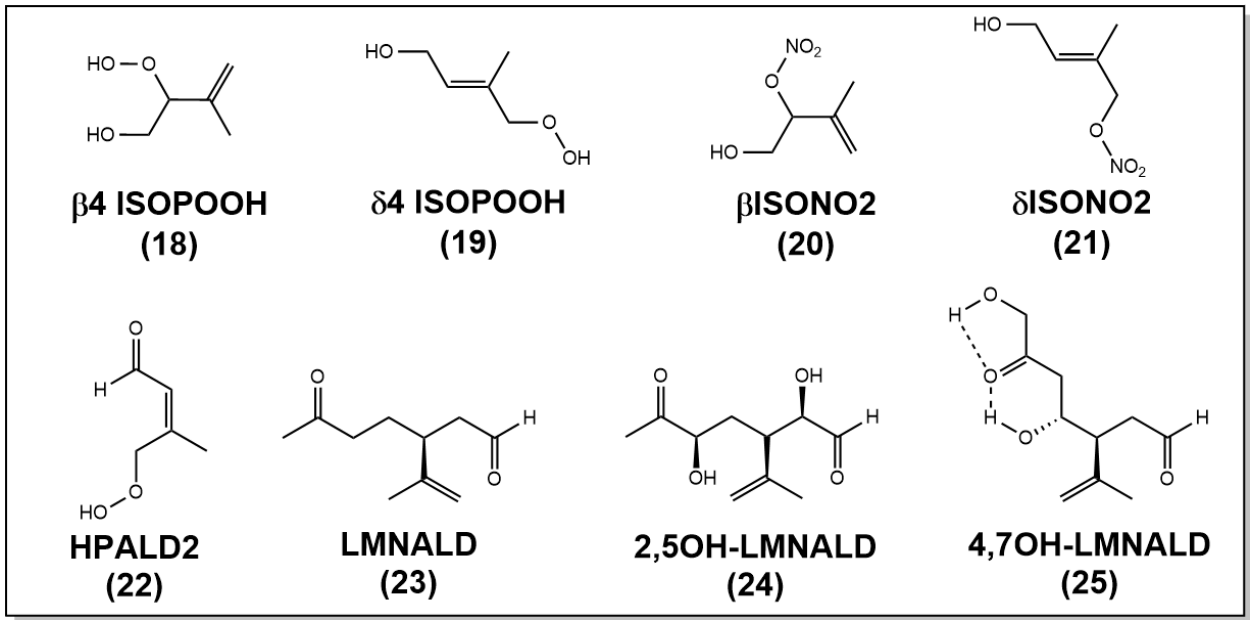

Figure S9. Lowest energy isomers of isoprene- and limonene-derived OVOCs, determined with gas-phase calculations using the CBS-QB3 compound method.

References

Canonica, S., Hellrung, B., and Wirz, J.: Oxidation of phenols by triplet aromatic ketones in aqueous solution, J. Phys. Chem. A, 104, 1226-1232, 2000.

Finlayson-Pitts, B. J., and Pitts Jr, J. N.: Chemistry of the Upper and Lower Atmosphere: Theory, Experiments, and Applications, Academic press, 1999.

Frisch, M., Trucks, G., Schlegel, H., Scuseria, G., Robb, M., Cheeseman, J., Scalmani, G., Barone, V., Petersson, G., Nakatsuji, H., Li, X., Caricato, M., Marenich, A., Bloino, J., Janesko, B., Gomperts, R., Mennucci, B., Hratchian, H., Ortiz, J., Izmaylov, A., Sonnenberg, J., Williams-Young, D., Ding, F., Lipparini, F., Egidi, F., Goings, J., Peng, B., Petrone, A., Henderson, T., Ranasinghe, D., Zakrzewski, V. G., Gao, J., Rega, N., Zheng, G., Liang, W., Hada, M., Ehara, M., Toyota, K., Fukuda, R., Hasegawa, J., Ishida, M., Nakajima, T., Honda, Y., Kitao, O., Nakai, H., Vreven, T., Throssell, K., J. A. Montgomery, J., Peralta, J. E., Ogliaro, F., Bearpark, M., Heyd, J. J., Brothers, E., Kudin, K. N., Staroverov, V. N., Keith, T., Kobayashi, R., Normand, J., Raghavachari, K., Rendell, A., Burant, J. C., Iyengar, S. S., Tomasi, J., Cossi, M., Millam, J. M., Klene, M., Adamo, C., CammI, R., Ochterski, J. W., Martin, R. L., Morokuma, K., Farkas, O., JB, F., and DJ, F.: Gaussian 09, Revision D.01; Gaussian: Wallingford, CT, USA, 2016,

Gill, K. J., and Hites, R. A.: Rate constants for the gas-phase reactions of the hydroxyl radical with isoprene, α-and β-pinene, and limonene as a function of temperature, The Journal of Physical Chemistry A, 106, 2538-2544, 2002.

Herrmann, H., Schaefer, T., Tilgner, A., Styler, S. A., Weller, C., Teich, M., and Otto, T.: Tropospheric aqueous-phase chemistry: Kinetics, mechanisms, and its coupling to a changing gas phase, Chem. Rev., 115, 4259-4334, 2015.

Jacobs, M. I., Burke, W., and Elrod, M. J.: Kinetics of the reactions of isoprene-derived hydroxynitrates: gas phase epoxide formation and solution phase hydrolysis, Atmos. Chem. Phys., 14, 8933-8946, 2014.

Kaur, R., and Anastasio, C.: Light absorption and the photoformation of hydroxyl radical and singlet oxygen in fog waters, Atmos. Environ., 164, 387-397, 2017.

Kaur, R., and Anastasio, C.: First Measurements of Organic Triplet Excited States in Atmospheric Waters, Environ. Sci. Technol., 52, 5218-5226, 2018.

Khamaganov, V. G., and Hites, R. A.: Rate Constants for the Gas-Phase Reactions of Ozone with Isoprene, α-and β-Pinene, and Limonene as a Function of Temperature, The Journal of Physical Chemistry A, 105, 815-822, 2001.

Lee, L., Teng, A. P., Wennberg, P. O., Crounse, J. D., and Cohen, R. C.: On Rates and Mechanisms of OH and O_3 Reactions with Isoprene-Derived Hydroxy Nitrates, The Journal of Physical Chemistry A, 118, 1622-1637, 2014.

Madronich, S., Flocke, S., Zeng, J., Petropavlovskikh, I., and Lee-Taylor, J.: Tropospheric Ultraviolet-Visible Model (TUV) version 4.1, National Center for Atmospheric Research, PO Box, 3000, 2002.

Richards-Henderson, N. K., Pham, A. T., Kirk, B. B., and Anastasio, C.: Secondary organic aerosol from aqueous reactions of green leaf volatiles with organic triplet excited states and singlet molecular oxygen, Environ. Sci. Technol., 49, 268-276, 2014.

Rivera-Rios, J. C., Zhao, R., Lee, A. K. Y., Abbatt, J. P. D., Crounse, J. D., Compernolle, S., Wennberg, P. O., and Keutsch, F. N.: In Preparation, 2018.

Schöne, L., and Herrmann, H.: Kinetic measurements of the reactivity of hydrogen peroxide and ozone towards small atmospherically relevant aldehydes, ketones and organic acids in aqueous solutions, Atmos. Chem. Phys., 14, 4503, 2014.

Schöne, L., Schindelka, J., Szeremeta, E., Schaefer, T., Hoffmann, D., Rudzinski, K. J., Szmigielski, R., and Herrmann, H.: Atmospheric aqueous phase radical chemistry of the isoprene oxidation products

methacrolein, methyl vinyl ketone, methacrylic acid and acrylic acid–kinetics and product studies, Phys. Chem. Chem. Phys., 16, 6257-6272, 2014.
Seinfeld, J. H., and Pandis, S. N.: Atmospheric chemistry and physics: From air pollution to climate change, John Wiley & Sons, 2012.
St. Clair, J. M., Rivera-Rios, J. C., Crounse, J. D., Knap, H. C., Bates, K. H., Teng, A. P., Jørgensen, S., Kjaergaard, H. G., Keutsch, F. N., and Wennberg, P. O.: Kinetics and Products of the Reaction of the First-Generation Isoprene Hydroxy Hydroperoxide (ISOPOOH) with OH, The Journal of Physical Chemistry A, 120, 1441-1451, 2015.
US EPA. Estimation Programs Interface Suite™ for Microsoft® Windows v 4.1: Estimation Programs Interface Suite™ for Microsoft® Windows, v 4.1. United States Environmental Protection Agency, Washington, DC, USA., 2016.
Witkowski, B., Al-sharafi, M., and Gierczak, T.: Kinetics of Limonene Secondary Organic Aerosol Oxidation in the Aqueous Phase, Environmental science & technology, 52, 11583-11590, 2018.
Wolfe, G. M., Crounse, J. D., Parrish, J. D., Clair, J. M. S., Beaver, M. R., Paulot, F., Yoon, T. P., Wennberg, P. O., and Keutsch, F. N.: Photolysis, OH Reactivity and Ozone Reactivity of a Proxy for Isoprene-Derived Hydroperoxyenals (HPALDs), Phys. Chem. Chem. Phys., 14, 7276-7286, 2012.